



Research paper

# Quantitative ab initio multireference investigation of the ground and low-lying electronic states of the diatomic molecule ScV

Magdalene Liosi, Aristotle Papakondylis\*

Department of Chemistry, Laboratory of Physical Chemistry, National and Kapodistrian University of Athens, Panepistimiopolis, Athens 157 71, Greece

## ARTICLE INFO

## Keywords:

Transition metal  
 Diatomic  
 ScV  
 MRCISD  
 Spectroscopic constants

## ABSTRACT

The lowest electronic states of the transition intermetallic ScV molecule have been studied by first principles employing the multireference configuration interaction technique and basis sets of quadruple- $\zeta$  quality. The ground state was found to be of  $X^7\Sigma^+$  symmetry with a binding energy of  $D_0^0 = 22.5$  kcal/mol relative to the ground separated atom limit and  $r_e = 2.571$  Å. Full potential energy curves were constructed for a total of 26 low-lying  $\Lambda$ -S states of ScV, extracting spectroscopic constants, as well. In addition, an effort was made to rationalize the nature of the chemical bond in the different states of the system.

## 1. Introduction

The study of transition intermetallic diatomics is, admittedly, a tough task challenging both experimentalists and theoreticians since at least four decades. Even for the “simpler” early first row transition diatomic molecules Sc<sub>2</sub>, ScTi, and Ti<sub>2</sub> a great effort was required in order to elucidate the electronic structure of their ground and excited states; see for instance refs [1–3]. Most of these species have relatively low binding energies and very often high-spin ground states. This is due, as is well known, to the much larger spatial extent of the 4s compared to the 3d orbitals, which prevents the shielded 3d electrons from effectively interacting covalently. Furthermore, most of the first row transition atoms have ground states with a  $3d^{n-2}4s^2$  valence electron distribution, where n is the number of valence electrons. As a result, all interactions between ground states with the  $4s^2$  configuration can only be of the van der Waals type (vdW). Bonding interactions should necessarily involve excited states of one or both transition atoms, with half-filled or empty 4s subshells. For example, the ground state of Sc<sub>2</sub> (of  $^5\Sigma_u^-$  symmetry) is formed [1] from the Sc( $^2D$ ) + Sc( $^4F$ ) combination with one of the two Sc atoms being in its first excited  $^4F(3d^24s^1)$  electronic state. The same stands for ScTi ( $X^6\Delta$ ) where the first excited  $^5F$  state of Ti is implicated [2]. For Ti<sub>2</sub> with a ground state of  $^3\Delta_g$  symmetry (nearly degenerate with a  $^1\Sigma_g^+$  state) it was shown [3] that both Ti atoms employ their first excited  $^5F$  state.

The formidable task of determining the ground state of a diatomic consisting of two transition metal atoms is the consequence of the

existence of many asymptotic channels closely packed together within a small energy interval of a few eV's, each channel giving rise to a multitude of molecular states with different spin and spatial symmetries. There is no strict rule allowing the precise prediction of the ground state symmetry as it is determined by many subtle factors.

Now, in this letter we present a systematic study of the low-lying electronic states of the ScV diatomic system. It is noteworthy, and also a motivation for this work, that no experimental or theoretical ab initio data could be found in the literature on this species. We are aware of only one DFT study by Gutsev et al. [4] who studied all ScM (M = Sc–Zn) dimer ground states. Using a generalized gradient approximation for the exchange–correlation potential and 6-311G\* basis sets, they found a  $X^7\Sigma^+$  ( $r_e = 2.513$  Å,  $D_e = 2.57$  eV,  $\omega_e = 246$  cm<sup>−1</sup>,  $\mu = 0.13$  D) ground state with a first excited state  $^3\Delta$  ( $r_e = 2.001$  Å,  $\omega_e = 342$  cm<sup>−1</sup>,  $\mu = 1.54$  D) just 0.10 eV higher. These results were also reported in a subsequent DFT paper by Gutsev et al. [5].

The ground atomic states of Sc( $^2D$ ) and V( $^4F$ ) with valence electronic distributions  $3d^14s^2$  and  $3d^34s^2$ , respectively, are not expected to lead to bonding interactions other than van der Waals. But what is interesting with the vanadium atom is that its first excited state,  $^6D(3d^44s^1)$ , is located only 0.25 eV [6] above its ground state. This is much lower than the Sc( $^4F;3d^24s^1$ ) state lying 1.44 eV [6] above its ground state. Thus, the asymptotic channel Sc( $^2D$ ) + V( $^6D$ ) is expected to play a key role in the formation of the lowest states of ScV. Indeed (vide infra), the majority of the 26 electronic states presently studied, trace their origin to the Sc( $^2D$ ) + V( $^6D$ ) asymptote.

The complexity of the problem can be realized by the number of  $\Lambda$ -S

\* Corresponding author.

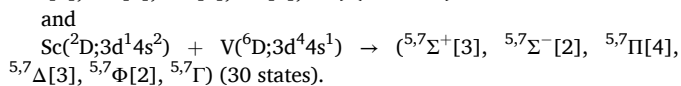
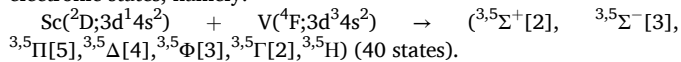
E-mail address: [papakondylis@chem.uoa.gr](mailto:papakondylis@chem.uoa.gr) (A. Papakondylis).<https://doi.org/10.1016/j.cplett.2025.141977>

Received 10 December 2024; Received in revised form 30 January 2025; Accepted 14 February 2025

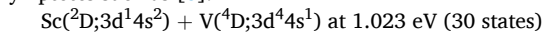
Available online 17 February 2025

0009-2614/© 2025 The Authors. Published by Elsevier B.V. This is an open access article under the CC BY license (<http://creativecommons.org/licenses/by/4.0/>).

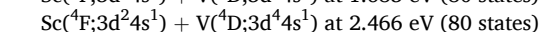
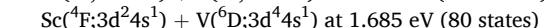
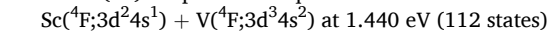
states arising from the two lowest atomic state combinations  $\text{Sc}(^2\text{D}) + \text{V}(^4\text{F})$  and  $\text{Sc}(^2\text{D}) + \text{V}(^6\text{D})$ ; they result in a total of  $70^{2S+1}\Lambda$  molecular electronic states, namely:



As mentioned before these two asymptotes are spaced by only 0.245 eV. Certainly, within a range of  $\sim 2.5$  eV one can find more atomic asymptotes such as [6]:



which resembles the  $\text{Sc}(^2\text{D}) + \text{V}(^6\text{D})$  asymptote but with the 5 electrons of  $\text{V}(^6\text{D})$  coupled into a quartet.



giving rise to a total of 372  $\Lambda$ -S states. In the present work, however, we only study low-lying states bound with respect to the ground  $\text{Sc}(^2\text{D}) + \text{V}(^4\text{F})$  asymptote, so only the  $\text{Sc}(^2\text{D}) + \text{V}(^4\text{D})$  channel intervenes in the formation of some triplets (see below).

The above numbers increase dramatically if we take into account the spin-orbit coupling, which, however, is not important for such light atoms and will not be considered in the present work.

In what follows we present a systematic multireference ab initio study of the 26 lowest bound states of ScV with a definitive assignment of its ground state. We report full potential energy curves (PEC), bond distances, binding energies, and spectroscopic constants accompanied by a discussion on the bonding characteristics of the different states.

## 2. Computational outline

For all calculated states and corresponding PECs the correlation consistent basis sets of quadruple cardinality, cc-pVQZ, were used for both atoms generally contracted to  $[8\text{s},7\text{p},5\text{d},3\text{f},2\text{g}]$  [7] comprising 186 contracted spherical Gaussians. For the ground state the quintuple cc-pV5Z basis contracted as  $[9\text{s},8\text{p},6\text{d},4\text{f},3\text{g},2\text{h}]$  [7] was employed, as well. For the relativistic Douglas-Kroll-Hess (DKH) [8,9] calculations we used the same basis sets, cc-pVQZ-DKH and cc-pV5Z-DKH, appropriately contracted.

Our computational approach was based on the internally contracted [10] multireference configuration interaction method, CASSCF+single+double replacements  $\equiv$  MRCI. The reference complete active space (CAS) was constructed by allotting the eight valence electrons ( $3\text{d}^14\text{s}^2 + 3\text{d}^34\text{s}^2$ ) of ScV to 15 orbitals correlating with the  $[4\text{s}(1) + 3\text{d}(5)]\times 2$  valence space of the Sc and V fragments supplemented with three orbitals of  $A_1$ ,  $B_1$ , and  $B_2$  symmetries (under  $C_{2v}$  restrictions). The latter three functions, at equilibrium, correspond to molecular orbitals centered on both atoms (see orbitals  $6a_1$ ,  $3b_1$ ,  $3b_2$  in the Supporting Information) and they provide greater flexibility to the active space. At infinity, they end up as 4p atomic orbitals of Sc and they contribute practically nothing. The size of the resulting CAS space under  $C_{2v}$  symmetry restrictions ranges from  $\sim 22.6 \times 10^3$  configuration state functions (CSF) for septets to  $\sim 107.3 \times 10^3$  (quintets) and to  $\sim 210 \times 10^3$  (triplets) CSFs. During the CASSCF optimization a number of states from all four irreducible representations ( $A_1, A_2, B_1, B_2$ ) were state averaged in order to assure a smooth evolution of the PECs along the internuclear distance and also correct  $\Lambda$  values. More specifically, states from  $A_1$  and  $A_2$  irreps were averaged for the description of  $\Sigma$ ,  $\Delta$ ,  $\Gamma$  molecular  $C_{\infty v}$  symmetries whilst  $B_1$  and  $B_2$  were used for the  $\Pi$  and  $\Phi$  states.

In the present calculations we did not consider the known double d-shell effect, (see for instance Ref. [11]) because it doesn't seem important for the Sc and V atoms. For example the  $[\text{V}(^4\text{F}) \leftarrow \text{V}(^6\text{D})]$  energy gap is very accurately predicted with the present computational scheme (vide infra).

In order to keep tractable the subsequent MRCI calculations the reference spaces were reduced by selecting only CSFs with the greatest CASSCF coefficients adding up to  $\sum |c_i|^2 = 0.9$  for each state. The resulting MRCI expansions contain  $10\text{-}15 \times 10^7$  CSFs internally contracted to  $7\text{-}10 \times 10^6$  CSFs. The absolute energy loss due to the reference space truncation was found to be  $\sim 3\text{-}5$  mE<sub>h</sub> for all states studied. Size non-extensivity was taken into account by applying the multireference Davidson correction [12] for unlinked quadruples, MRCI+Q.

Spectroscopic constants were extracted by numerically solving the nuclear Schrödinger equation using a Numerov procedure with a code developed in our laboratory and employing the masses of the  $^{45}\text{Sc}$  and  $^{51}\text{V}$  isotopes.

All electronic structure calculations were carried out with the MOLPRO program [13,14].

## 3. Results and discussion

Table 1 collects the numerical data obtained for 26 electronic states of ScV while Figs. 1, 2, and 3 display the corresponding PECs for spin multiplicities 7, 5, and 3, respectively. The different states are numbered in ascending order of their absolute electronic energies as obtained at the MRCI level.

From our previous analysis we see that the ground state atomic asymptote  $\text{Sc}(^2\text{D}) + \text{V}(^4\text{F})$  can give rise to triplets and quintets while the first excited  $\text{Sc}(^2\text{D}) + \text{V}(^6\text{D})$  asymptote gives quintets and septets. Now, from Table 1 it is clear that the ground state of ScV is of  $X^7\Sigma^+$  symmetry. We discuss first septet states then the quintets and finally the triplets.

### 3.1. Septets

The ground state of the ScV diatomic is of  $X^7\Sigma^+$  symmetry originating adiabatically from the first excited asymptotic channel  $\text{Sc}(^2\text{D}) + \text{V}(^6\text{D})$ , Fig. 1. The bonding occurs mainly through a two center-three electron (2c-3e) interaction,  $4\text{s}^2\text{-}4\text{s}^1$ , with minor 3d-3d contributions. The equilibrium MRCI wave function is dominated by the configuration

$$|(\text{core})1\sigma^2 2\sigma^1 3\sigma^1 1\pi_+^1 1\pi_-^1 1\delta_+^1 1\delta_-^1 \rangle$$

(where only valence orbitals are counted) with a coefficient of 0.85. The corresponding atomic Mulliken electronic distributions at equilibrium are:

$$4\text{s}^{1.77} 4\text{p}_z^{0.38} 4\text{p}_x^{0.07} 4\text{p}_y^{0.07} 3\text{d}_{z^2}^{0.29} 3\text{d}_{xz}^{0.42} 3\text{d}_{yz}^{0.42} 3\text{d}_{x^2-y^2}^{0.03} 3\text{d}_{xy}^{0.02} / \text{Sc}(-0.47)$$

$$4\text{s}^{0.60} 4\text{p}_z^{0.12} 4\text{p}_x^{0.06} 4\text{p}_y^{0.06} 3\text{d}_{z^2}^{0.75} 3\text{d}_{xz}^{0.51} 3\text{d}_{yz}^{0.51} 3\text{d}_{x^2-y^2}^{0.96} 3\text{d}_{xy}^{0.96} / \text{V}(+0.47)$$

These populations coupled to the orbitals participating in the leading configuration refer to a bonding situation which can be depicted by Scheme 1.

In this scheme the d orbitals are represented by overextended sticks in order to clearly show the formal interactions between them. Of course the main bonding comes from the much more diffuse  $4\text{s}^2\text{-}4\text{s}^1$  approach which gives rise to a two-electron  $\sigma$  bond ( $1\sigma^2$ ) with the third electron promoted to a non-bonding orbital ( $2\sigma^1$ ). We must say here that the problem of 2c-3e bonds is still an open debate among chemists (see for instance Ref. [15]). However, in our case and in terms of molecular orbitals, according to our calculations, the three electron interaction can be illustrated by Scheme 2. In this scheme we can clearly see the non-bonding nature of the  $2\sigma$  orbital. We also remark that its corresponding Fock energy was found  $-0.077$  E<sub>h</sub> which means that the  $2\sigma^1$  electron is well bound to the system. See, also, the figures of the  $1\sigma$  and  $2\sigma$  orbitals in the Supporting Information file.

From the Mulliken populations we observe partial electron transfers between  $d_{xz}$ ,  $d_{yz}$  and  $d_{z^2}$  atomic orbitals of the two atoms while the  $\delta$  orbitals are completely localized on V ( $d_{x^2-y^2}$  and  $d_{xy}$  with coefficients of 0.99). There is an overall  $0.47$  e<sup>-</sup> transfer from V to Sc which mainly

**Table 1**

Energy  $E$  ( $E_h$ ), Bond length  $r_e$  (Å), Binding energies  $D_e, D_0$  (kcal/mol), Harmonic Frequency  $\omega_e$  ( $\text{cm}^{-1}$ ), Anharmonicity Constant  $\omega_e x_e$  ( $\text{cm}^{-1}$ ), Centrifugal Distortion Constant  $\bar{D}_e$  ( $\text{cm}^{-1}$ ), Rotation-Vibration Coupling Constant  $a_e$  ( $\text{cm}^{-1}$ ), Net Mulliken Charge  $q_{\text{Sc}}$  (e) on Sc, Dipole Moment  $\mu$  (D) and Energy Separations  $T_e$  ( $\text{cm}^{-1}$ ) for 26 Low-Lying Electronic States of ScV at the MRCI(+Q)/cc-pVQZ Level of Theory.

| Method                                  | $-E$       | $r_e$ | $D_e^a$ | $D_0^a$ | $\omega_e$ | $\omega_e x_e$ | $\bar{D}_e (\times 10^{-7})$ | $a_e (\times 10^{-3})$ | $q_{\text{Sc}}$ | $\mu$ | $T_e$ |
|---|------------|-------|---------|---------|------------|----------------|------------------------------|------------------------|-----------------|-------|-------|
| <b><math>X^2\Sigma^+</math></b>         |            |       |         |         |            |                |                              |                        |                 |       |       |
| MRCI                                    | 1702.76658 | 2.605 | 22.9    | 22.6    | 205        | 1.062          | 1.00                         | 0.55                   | -0.47           | 0.17  | 0.0   |
| MRCI+Q                                  | 1702.7751  | 2.600 | 25.8    | 25.6    | 208        | 0.989          | 0.99                         | 0.58                   |                 |       | 0.0   |
| MRCI-DKH <sup>b</sup>                   | 1711.59136 | 2.577 | 26.7    | 26.4    | 223        |                |                              |                        | -0.43           | 0.25  | 0.0   |
| MRCI-DKH + Q <sup>b</sup>               | 1711.5991  | 2.575 | 28.0    | 27.6    | 254        |                |                              |                        |                 |       | 0.0   |
| MRCI(5 $\zeta$ ) <sup>c</sup>           | 1702.77149 | 2.596 | 21.5    | 21.2    | 210        |                |                              |                        | -0.26           | 0.20  | 0.0   |
| MRCI(5 $\zeta$ ) + Q <sup>c</sup>       | 1702.7794  | 2.591 | 25.5    | 25.2    | 213        |                |                              |                        |                 |       | 0.0   |
| MRCI(5 $\zeta$ )-DKH <sup>b,c</sup>     | 1711.59447 | 2.574 | 27.1    | 26.8    | 225        |                |                              |                        | -0.26           | 0.27  | 0.0   |
| MRCI(5 $\zeta$ )-DKH + Q <sup>b,c</sup> | 1711.6024  | 2.571 | 28.5    | 28.2    | 232        |                |                              |                        |                 |       | 0.0   |
| <b><math>1^5\Pi</math></b>              |            |       |         |         |            |                |                              |                        |                 |       |       |
| MRCI                                    | 1702.75747 | 2.637 | 11.5    | 11.2    | 173        | 8.110          | 1.50                         | -0.68                  | -0.36           | 0.34  | 1999  |
| MRCI+Q                                  | 1702.7687  | 2.607 | 15.1    | 14.9    | 142        | -10.892        | 3.01                         | -1.26                  |                 |       | 1405  |
| <b><math>2^7\Sigma^-</math></b>         |            |       |         |         |            |                |                              |                        |                 |       |       |
| MRCI                                    | 1702.75686 | 2.928 | 16.7    | 16.5    | 175        | 0.777          | 0.99                         | 0.75                   | -0.14           | 0.14  | 2133  |
| MRCI+Q                                  | 1702.7642  | 2.927 | 19.1    | 18.9    | 179        | 0.927          | 0.79                         | 0.46                   |                 |       | 2392  |
| <b><math>3^5\Phi</math></b>             |            |       |         |         |            |                |                              |                        |                 |       |       |
| MRCI                                    | 1702.75651 | 2.671 | 10.9    | 10.6    | 153        | 0.099          | 1.53                         | 1.10                   | -0.38           | 0.36  | 2210  |
| MRCI+Q                                  | 1702.7677  | 2.650 | 14.4    | 14.2    | 151        | 0.201          | 1.98                         | -0.71                  |                 |       | 1624  |
| <b><math>4^7\Gamma</math></b>           |            |       |         |         |            |                |                              |                        |                 |       |       |
| MRCI                                    | 1702.75643 | 2.948 | 16.4    | 16.2    | 172        | 0.690          | 0.74                         | 0.44                   | -0.18           | 0.49  | 2228  |
| MRCI+Q                                  | 1702.7639  | 2.931 | 18.9    | 18.7    | 176        | 0.555          | 0.75                         | 0.49                   |                 |       | 2458  |
| <b><math>5^5\Delta</math></b>           |            |       |         |         |            |                |                              |                        |                 |       |       |
| MRCI                                    | 1702.75589 | 2.800 | 10.3    | 10.0    | 172        | -1.028         | -0.138                       | 0.281                  | -0.30           | 0.10  | 2346  |
| MRCI+Q                                  | 1702.7668  | 2.802 | 14.0    | 13.7    | 233        | 24.434         | 0.131                        | -0.965                 |                 |       | 1821  |
| <b><math>6^7\Phi</math></b>             |            |       |         |         |            |                |                              |                        |                 |       |       |
| MRCI                                    | 1702.75533 | 2.919 | 16.4    | 16.1    | 172        | 0.388          | 0.57                         | 0.77                   | -0.14           | 0.03  | 2469  |
| MRCI+Q                                  | 1702.7626  | 2.906 | 17.8    | 17.5    | 179        | 1.873          | 0.58                         | 0.62                   |                 |       | 2743  |
| <b><math>7^7\Pi</math></b>              |            |       |         |         |            |                |                              |                        |                 |       |       |
| MRCI                                    | 1702.75401 | 2.948 | 15.5    | 15.3    | 167        | 0.138          | 0.55                         | 0.64                   | -0.14           | 0.04  | 2759  |
| MRCI+Q                                  | 1702.7613  | 2.938 | 16.9    | 16.6    | 178        | 2.489          | 0.62                         | 0.66                   |                 |       | 3029  |
| <b><math>8^3\Pi</math></b>              |            |       |         |         |            |                |                              |                        |                 |       |       |
| MRCI                                    | 1702.75225 | 2.650 | 8.2     | 8.0     | 177        | 7.319          | 1.10                         | 0.05                   | -0.35           | 0.51  | 3145  |
| MRCI+Q                                  | 1702.7637  | 2.623 | 11.9    | 11.6    | 165        | -5.369         | 1.60                         | 3.82                   |                 |       | 2502  |
| <b><math>9^7\Delta</math></b>           |            |       |         |         |            |                |                              |                        |                 |       |       |
| MRCI                                    | 1702.75167 | 2.950 | 13.2    | 13.0    | 167        | 0.450          | 0.77                         | 0.51                   | -0.20           | 0.11  | 3272  |
| MRCI+Q                                  | 1702.7600  | 2.927 | 16.0    | 15.8    | 178        | 0.899          | 0.66                         | 0.48                   |                 |       | 3314  |
| <b><math>10^3\Phi</math></b>            |            |       |         |         |            |                |                              |                        |                 |       |       |
| MRCI                                    | 1702.75144 | 2.653 | 7.7     | 7.4     | 172        | 3.733          | 0.84                         | 0.51                   | -0.35           | 0.51  | 3323  |
| MRCI+Q                                  | 1702.7627  | 2.650 | 11.3    | 11.1    | 151        | -7.773         | 2.15                         | 3.08                   |                 |       | 2721  |
| <b><math>11^5\Gamma</math></b>          |            |       |         |         |            |                |                              |                        |                 |       |       |
| MRCI                                    | 1702.75117 | 2.943 | 7.4     | 7.1     | 168        | -9.766         | 0.83                         | -0.90                  | -0.19           | 0.46  | 3382  |
| MRCI+Q                                  | 1702.7621  | 2.950 | 10.8    | 10.5    | 217        | 8.307          | 0.60                         | -3.31                  |                 |       | 2853  |
| <b><math>12^3\Delta</math></b>          |            |       |         |         |            |                |                              |                        |                 |       |       |
| MRCI                                    | 1702.75116 | 2.173 | 7.4     | 7.0     | 284        | -1.379         | 2.00                         | -2.13                  | -1.15           | 1.36  | 3384  |
| MRCI+Q                                  | 1702.7616  | 2.170 | 10.5    | 10.1    | 280        | 4.768          | 1.66                         | 1.07                   |                 |       | 2963  |
| <b><math>13^5\Sigma^+</math></b>        |            |       |         |         |            |                |                              |                        |                 |       |       |
| MRCI                                    | 1702.75095 | 2.944 | 7.1     | 6.9     | 182        | -3.507         | 0.23                         | -0.63                  | -0.19           | 0.48  | 3430  |
| MRCI+Q                                  | 1702.7617  | 2.950 | 10.4    | 10.1    | 223        | 10.723         | 1.54                         | -2.41                  |                 |       | 2941  |
| <b><math>14^5\Sigma^-</math></b>        |            |       |         |         |            |                |                              |                        |                 |       |       |

(continued on next page)

Table 1 (continued)

| Method                             | $-E$       | $r_e$ | $D_e^a$ | $D_0^a$ | $\omega_e$ | $\omega_e x_e$ | $\bar{D}_e (\times 10^{-7})$ | $a_e (\times 10^{-3})$ | $q_{sc}$ | $\mu$ | $T_e$ |
|------------------------------------|------------|-------|---------|---------|------------|----------------|------------------------------|------------------------|----------|-------|-------|
| MRCI                               | 1702.75089 | 2.950 | 7.1     | 6.8     | 182        | -2.915         | 0.65                         | -1.40                  | -0.19    | 0.46  | 3444  |
| MRCI+Q                             | 1702.7618  | 2.931 | 10.5    | 10.1    | 221        | 9.711          | 0.27                         | -2.34                  |          |       | 2919  |
| <b>15<sup>7</sup>Φ</b>             |            |       |         |         |            |                |                              |                        |          |       |       |
| MRCI                               | 1702.74874 | 3.114 | 12.2    | 12.0    | 149        | 0.944          | 0.47                         | 0.49                   | -0.14    | 0.61  | 3915  |
| MRCI+Q                             | 1702.7562  | 3.097 | 14.4    | 14.2    | 155        | 0.918          | 0.84                         | 0.46                   |          |       | 4148  |
| <b>16<sup>7</sup>Σ<sup>+</sup></b> |            |       |         |         |            |                |                              |                        |          |       |       |
| MRCI                               | 1702.74838 | 2.925 | 11.4    | 11.2    | 149        | 1.096          | 0.80                         | 0.96                   | -0.14    | 0.20  | 3994  |
| MRCI+Q                             | 1702.7591  | 2.856 | 15.9    | 15.7    | 194        | 3.150          | 0.75                         | 0.98                   |          |       | 3512  |
| <b>17<sup>7</sup>Π</b>             |            |       |         |         |            |                |                              |                        |          |       |       |
| MRCI                               | 1702.74814 | 3.133 | 11.9    | 11.6    | 146        | 0.927          | 0.67                         | 0.42                   | -0.14    | 0.61  | 4047  |
| MRCI+Q                             | 1702.7556  | 3.111 | 14.1    | 13.8    | 152        | 0.654          | 0.48                         | 0.40                   |          |       | 4280  |
| <b>18<sup>5</sup>Π</b>             |            |       |         |         |            |                |                              |                        |          |       |       |
| MRCI                               | 1702.74813 | 2.291 | 5.2     | 4.7     | 335        | 13.297         | 0.83                         | 5.15                   | -0.82    | 1.28  | 4049  |
| MRCI+Q                             | 1702.7606  | 2.300 | 10.0    | 9.5     | 365        | 11.038         | 0.57                         | 7.31                   |          |       | 3182  |
| <b>19<sup>7</sup>Δ</b>             |            |       |         |         |            |                |                              |                        |          |       |       |
| MRCI                               | 1702.74659 | 3.151 | 10.1    | 9.9     | 141        | 0.831          | 0.74                         | 0.47                   | -0.20    | 0.11  | 4387  |
| MRCI+Q                             | 1702.7552  | 3.090 | 13.1    | 12.9    | 154        | 1.489          | 0.66                         | 0.49                   |          |       | 4368  |
| <b>20<sup>3</sup>Σ<sup>+</sup></b> |            |       |         |         |            |                |                              |                        |          |       |       |
| MRCI                               | 1702.74514 | 2.942 | 3.5     | 3.3     | 180        | -              | -                            | -                      | -0.11    | 1.16  | 4706  |
| MRCI+Q                             | 1702.7581  | 2.929 | 8.2     | 8.0     | 142        |                |                              |                        |          |       | 3731  |
| <b>21<sup>3</sup>Γ</b>             |            |       |         |         |            |                |                              |                        |          |       |       |
| MRCI                               | 1702.74486 | 2.944 | 3.4     | 3.1     | 180        | -              | -                            | -                      | -0.11    | 1.15  | 4767  |
| MRCI+Q                             | 1702.7586  | 2.921 | 8.5     | 8.2     | 186        |                |                              |                        |          |       | 3621  |
| <b>22<sup>3</sup>Σ<sup>-</sup></b> |            |       |         |         |            |                |                              |                        |          |       |       |
| MRCI                               | 1702.74481 | 2.949 | 3.3     | 3.1     | 156        | -              | -                            | -                      | -0.13    | 0.97  | 4778  |
| MRCI+Q                             | 1702.7583  | 2.908 | 8.3     | 8.2     | 125        |                |                              |                        |          |       | 3687  |
| <b>23<sup>5</sup>Φ</b>             |            |       |         |         |            |                |                              |                        |          |       |       |
| MRCI                               | 1702.74279 | 2.850 | 2.2     | 2.0     | 163        | -4.308         | 1.28                         | 1.84                   | -0.16    | 1.29  | 5221  |
| MRCI+Q                             | 1702.7541  | 2.850 | 5.9     | 5.6     | 179        | 2.135          | 0.83                         | 1.49                   |          |       | 4609  |
| <b>24<sup>7</sup>Π</b>             |            |       |         |         |            |                |                              |                        |          |       |       |
| MRCI                               | 1702.74231 | 3.146 | 8.2     | 8.1     | 126        | 1.423          | 0.98                         | 1.14                   | -0.16    | 0.22  | 5327  |
| MRCI+Q                             | 1702.7520  | 3.057 | 11.4    | 11.1    | 148        | 1.455          | 0.84                         | 1.58                   |          |       | 5070  |
| <b>25<sup>7</sup>Π</b>             |            |       |         |         |            |                |                              |                        |          |       |       |
| MRCI                               | 1702.74148 | 3.136 | 7.7     | 7.5     | 136        | 1.474          | 0.64                         | 1.04                   | -0.16    | 0.52  | 5509  |
| MRCI+Q                             | 1702.7510  | 3.060 | 10.8    | 10.5    | 152        | 1.119          | 0.57                         | 1.42                   |          |       | 5289  |

<sup>a</sup> Binding energies with respect to  $Sc(^2D) + V(^6D)$  for all septet states and with respect to  $Sc(^2D) + V(^4F)$  for all other states.

<sup>b</sup> With scalar relativistic Douglas-Kroll-Hess (DKH) corrections of third order.

<sup>c</sup> Calculations with the cc-pV5Z basis sets.

happens in the  $\sigma$ -frame of the system. However, the low dipole moment value of 0.17 D, Table 1, does not account for such a significant charge transfer. This number was calculated as an expectation value. Using the finite field method by applying weak electric fields and extrapolating to zero field, we found  $\mu = 0.30$  D which is rather low, as well. Of course Mulliken charges only show tendencies not real charges.

The binding energy of  $ScV(X^7\Sigma^+)$ , with respect to its adiabatic asymptote  $Sc(^2D) + V(^6D)$ , was found  $D_e = 25.8(25.5)$  kcal/mol at the MRCI+Q/cc-pVQZ(cc-pV5Z) levels of theory. This value increases by 2–3 kcal/mol with the addition of scalar relativistic corrections, MRCI+DKH+Q, Table 1. The equilibrium bond length was found  $r_e = 2.57$ – $2.60$  Å depending on the different methods used. At this point it is interesting to report also some RCCSD(T)/cc-pVQZ(cc-pV5Z) results for the ground state, namely,  $r_e = 2.578$  (2.576) Å,  $D_e = 19.7$  (20.6) kcal/mol,  $\omega_e = 223$  (226)  $cm^{-1}$ . Nevertheless, these numbers are to be taken with some caution since the  $X^7\Sigma^+$  state is not of a purely single reference

nature, as indicated by the relatively large  $T_1 = 0.128$  diagnostic (see for example Ref. [17]).

We must note here the striking differences between our results and the DFT numbers,  $D_e = 2.57$  eV (= 59.3 kcal/mol) and  $r_e = 2.51$  Å, by Gutsev et al. [4,5]. However, we have the conviction that our mutireference calculations provide the correct numbers.

The binding energy is rather low, which is typical for 2c-3e interactions. It yields a  $D_0^b = 22.5$  kcal/mol with respect to the ground state fragments  $Sc(^2D) + V(^4F)$  at the MRCI+DKH+Q/cc-pV5Z level of theory. Note that the energy gap  $\Delta E[V(^4F) \leftarrow V(^6D)]$  was calculated at all levels  $\Delta E = 0.009 E_h = 1975 cm^{-1}$  in excellent agreement with the experimental ( $M_J$ -averaged) value  $\Delta E = 1977 cm^{-1}$  [6].

Fig. 1 shows PECs for 10 additional septet states stemming from the  $Sc(^2D) + V(^6D)$  asymptote. The bonding mode for these states is basically the same as in the ground state; the 2c-3e interaction ( $4s^2-4s^1$ ) prevails and their relative positions are determined by the weaker 3d-3d

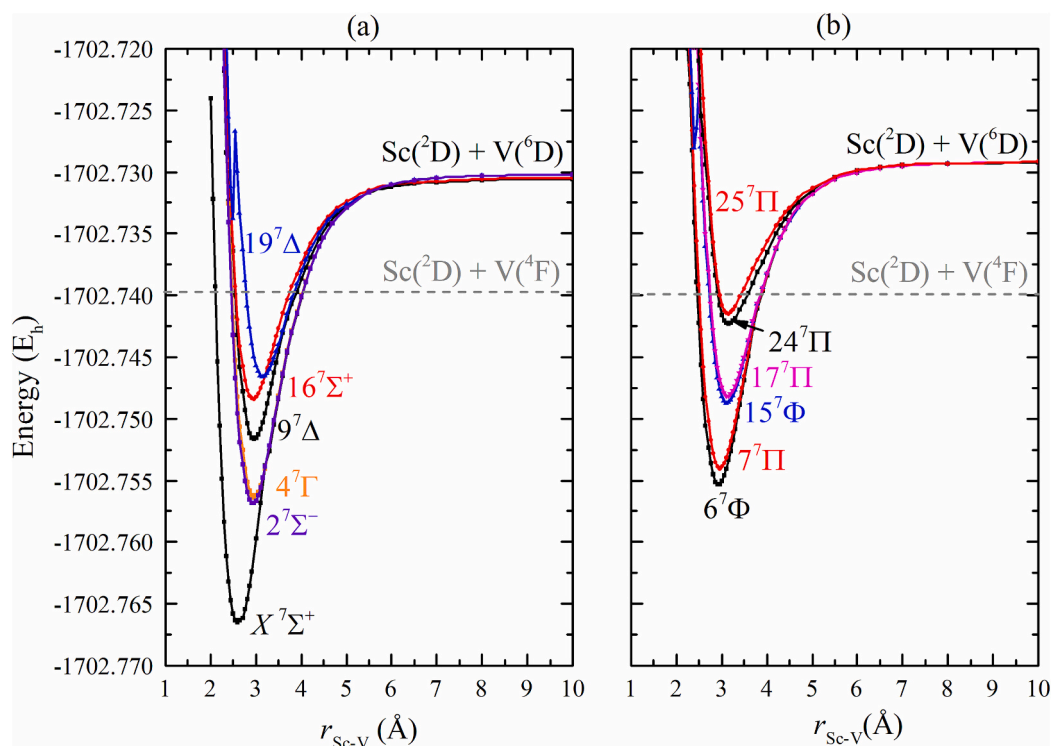


Fig. 1. Potential energy curves of the twelve lowest septet states of ScV at the MRCI/cc-pVQZ level of theory: (a)  $X^7\Sigma^+$ ,  $2^7\Sigma^-$ ,  $4^7\Gamma$ ,  $9^7\Delta$ ,  $16^7\Sigma^+$ ,  $19^7\Delta$ , and (b)  $6^7\Phi$ ,  $7^7\Pi$ ,  $15^7\Phi$ ,  $17^7\Pi$ ,  $24^7\Pi$ ,  $25^7\Pi$ .

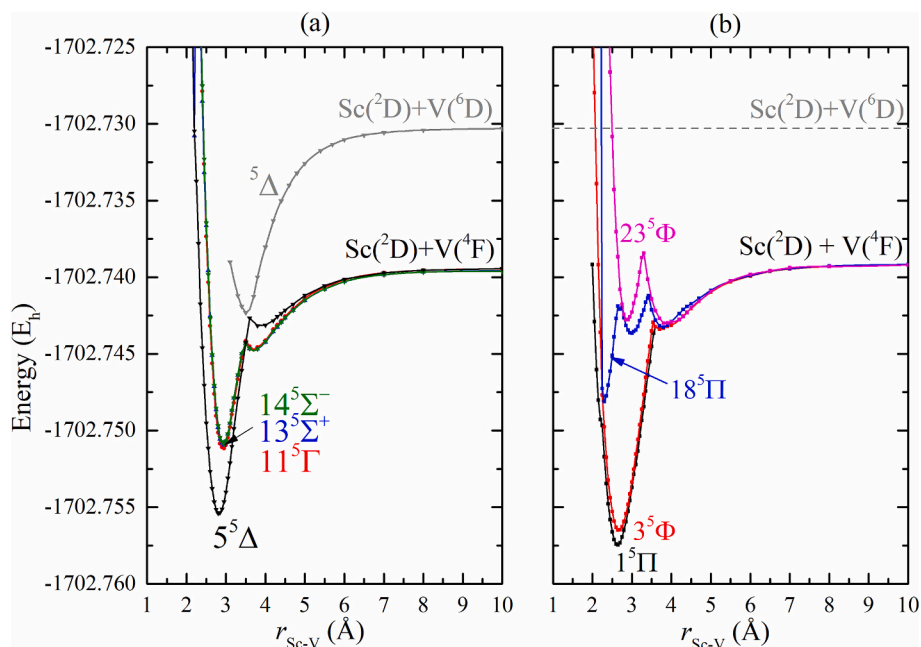


Fig. 2. Potential energy curves of the eight lowest quintet states of ScV at the MRCI/cc-pVQZ level of theory: (a)  $5^5\Delta$ ,  $11^5\Gamma$ ,  $13^5\Sigma^+$ ,  $14^5\Sigma^-$  and (b)  $1^5\Pi$ ,  $3^5\Phi$ ,  $18^5\Pi$ ,  $23^5\Phi$ .

interactions. As we can see from Table 1 they are interlaced with other states of quintuple spin multiplicity within a narrow energy window of  $\sim 3000\text{ cm}^{-1}$ . In some cases of near-degeneracy the ordering based on the MRCI energies is reversed at the MRCI+Q level.

### 3.2. Quintets

Table 1 shows that the first excited state of the ScV system is of  $5^5\Pi$

symmetry with  $T_e = 1999(1405)\text{ cm}^{-1}$  at the MRCI(+Q) levels. This is in contrast with the results of Gutsev et al. [4] predicting a  $3^5\Delta$  as first excited state with  $T_e = \sim 800\text{ cm}^{-1}$ . Very close to  $1^5\Pi$ , within a range of  $\sim 500\text{ cm}^{-1}$ , there are also other states like  $2^7\Sigma^-$ ,  $3^5\Phi$ ,  $4^7\Gamma$ ,  $5^5\Delta$ , and  $6^7\Phi$ , Table 1. The binding energy of  $1^5\Pi$  was computed at the MRCI+Q/cc-pVQZ level as  $D_e = 15.1\text{ kcal/mol}$  with respect to the ground state asymptote  $\text{Sc}(2D) + \text{V}(4F)$ .

Fig. 2 displays PECs for eight bound, with respect to the ground

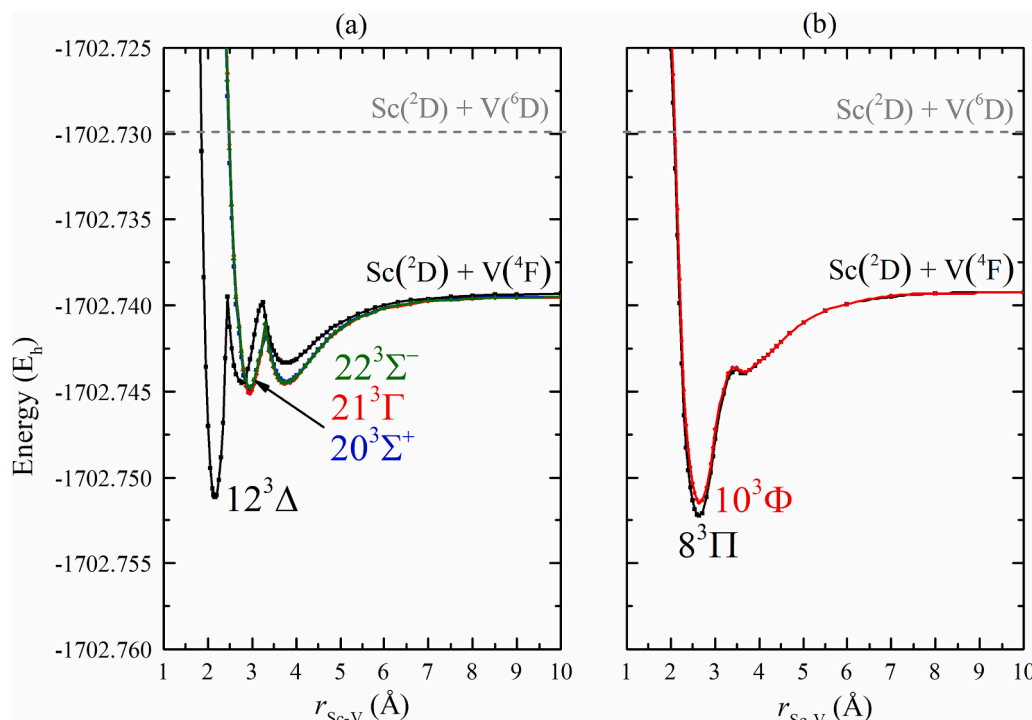
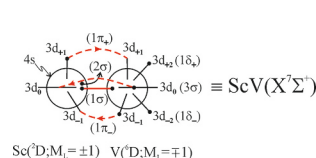
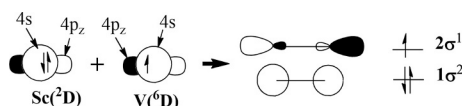


Fig. 3. Potential energy curves of the six lowest triplet states of ScV at the MRCI/cc-pVQZ level of theory: (a)  $12^3\Delta$ ,  $20^3\Sigma^+$ ,  $21^3\Gamma$ ,  $22^3\Sigma^-$  and (b)  $8^3\Pi$ , and  $10^3\Phi$ .



Scheme 1.



Scheme 2.

asymptote, quintet states of ScV. They all adiabatically correlate to the  $\text{Sc}(^2D) + \text{V}(^4F)$  atomic channel. However, we observe that after forming shallow vdW minima at  $\sim 3.80\text{--}4.00 \text{ \AA}$ , they all suffer an abrupt change indicative of an avoided crossing. This is clearly illustrated in Fig. 2a where it is shown how the  $5^5\Delta$  state non-adiabatically traces its lineage to the  $\text{Sc}(^2D) + \text{V}(^6D)$  asymptote by crossing the lower  $^5\Delta$  PEC at  $r(\text{Sc}-\text{V}) = 3.60 \text{ \AA}$ . This quasi-diabatic curve was produced by a reference CASSCF accidentally locked in its equilibrium configuration. Thus, the in situ equilibrium electronic distribution corresponds to the first excited atomic configuration  $\text{Sc}(^2D) + \text{V}(^6D)$ . From Fig. 2 we observe the same features for all quintet PECs. We will discuss now in some detail the first excited  $1^5\Pi$  state.

At equilibrium, its MRCI wave function is basically characterized by the following CSF:

$$0.48 |(\text{core})1\sigma^2 2\sigma^1 3\sigma^1 1\pi_x^2 1\pi_y^1 1\delta_{xy}^1\rangle -$$

$$0.48 |(\text{core})1\sigma^2 2\sigma^1 3\sigma^1 1\pi_x^1 1\pi_y^2 1\delta_{x^2-y^2}^1\rangle$$

corresponding to the  $B_1$  component. The Mulliken atomic populations are:

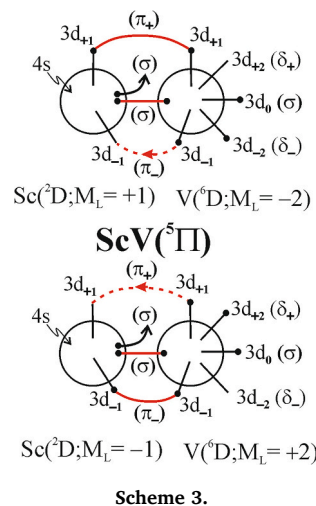
$$4s^{1.60} 4p_z^{0.40} 4p_x^{0.07} 4p_y^{0.07} 3d_{z^2}^{0.10} 3d_{xz}^{0.70} 3d_{yz}^{0.42} 3d_{x^2-y^2}^{0.00} 3d_{xy}^{0.00} / \text{Sc}(-0.36)$$

$$4s^{0.75} 4p_z^{0.15} 4p_x^{0.06} 4p_y^{0.06} 3d_{z^2}^{0.90} 3d_{xz}^{0.90} 3d_{yz}^{0.77} 3d_{x^2-y^2}^{0.35} 3d_{xy}^{0.70} / \text{V}(+0.36)$$

denoting a  $\sim \text{Sc}(3d^1 4s^2) + \text{V}(3d^4 4s^1)$  atomic in situ electronic configuration. Taking into account and the  $B_2$  component, the bonding in the  $\text{ScV}(1^5\Pi)$  state can be described by Scheme 3.

In this scheme we can see that in addition to the  $(4s^2-4s^1)$  interaction we have one and a half formal  $\pi$ -bonds involving 3d orbitals and supplementing the overall bonding. It is interesting at this point to evaluate the contribution of these  $\pi$ -bonds. An estimate of the strength of the 2-electron  $d_x$  bond can be found by comparison of  $1^5\Pi$  with the  $7^7\Pi$  state. The latter can also be described by Scheme 3 but with the  $d_x^2$  bond broken by uncoupling the two electrons. As a result,  $7^7\Pi$  finds itself  $\sim 3.5$  (7.0)  $mE_h$  higher than  $1^5\Pi$  at the MRCI(+Q) level, Table 1. This yields a contribution of  $\sim 2\text{--}4 \text{ kcal/mol}$  to the overall bonding of the  $1^5\Pi$  state.

All other quintet states presented in Fig. 2 are formed through a similar mechanism involving also the first excited asymptote and have very low binding energies. There is an exception with state  $18^5\Pi$  which in addition to the minimum at  $\sim 3 \text{ \AA}$  (Fig. 2) coming from the  $\text{Sc}(^2D) + \text{V}$



Scheme 3.

(<sup>6</sup>D) channel, it shows a second minimum at a much shorter distance  $r_e = 2.300 \text{ \AA}$  (Fig. 2b). This is its global minimum and although it has a very low binding energy with respect to the ground state asymptote, it is worth mentioning that unlike the other quintets it has a rather strong ionic character ( $\mu = 1.28 \text{ D}$ ,  $q_{\text{Sc}} = -0.82$ , Table 1) and undoubtedly stems from a higher asymptote.

### 3.3. Triplets

Fig. 3 shows PECs for 6 triplet states correlating adiabatically to the ground state  $\text{Sc}(^2\text{D}) + \text{V}(^4\text{F})$  asymptote. They all have very small binding energy values, Table 1. Apart from their characteristic vdW minima at  $\sim 3.80 \text{ \AA}$ , they all possess additional potential wells resulting from avoided crossings with higher incoming PECs. Since the first excited atomic channel,  $\text{Sc}(^2\text{D}) + \text{V}(^6\text{D})$ , cannot form triplet states we conclude that they originate from  $\text{Sc}(^2\text{D}) + \text{V}(^4\text{D})$  lying  $1.023 \text{ eV}$  above the ground state [6]. For instance the in situ electronic configuration of the  $8^3\Pi$  state (Fig. 3b) can be depicted by Scheme 3 but with the four single electrons coupled into a triplet. Now, a word must be said concerning the  $12^3\Delta$  state. As we can see from Fig. 3a its PEC forms a third (global) minimum in addition to the vdW minimum and the one coming from the  $\text{Sc}(^2\text{D}) + \text{V}(^4\text{D})$  asymptote. Our analysis shows an ionic state with a dipole moment of  $1.36 \text{ D}$  (Table 1). Just like  $18^5\Pi$  mentioned before this state must non-adiabatically correlate to a higher asymptote. It has a much shorter bond length,  $r_e = 2.17 \text{ \AA}$ , and is located  $\sim 0.4 \text{ eV}$  above the ground  $X^7\Sigma^+$  state of ScV, much higher as compared to the value of  $0.1 \text{ eV}$  of Ref. [5].

## 4. Summary and conclusions

We have employed the multireference complete active space MRCISD methodology in conjunction with high quality correlation consistent basis sets to study 26 low-lying  $\Lambda$ -S electronic states of the ScV diatomic system.

For the first time full potential energy curves were constructed for all states considered, and corresponding spectroscopic constants were extracted.

The ground state was unambiguously found to be of  $X^7\Sigma^+$  symmetry. It correlates adiabatically to the  $\text{Sc}(^2\text{D}) + \text{V}(^6\text{D})$  asymptotic channel with a recommended  $D_0 = 28 \text{ kcal/mol}$  binding energy relative to that limit which yields a  $D_0^0 = 22.5 \text{ kcal/mol}$  value with respect to the  $\text{Sc}(^2\text{D}) + \text{V}(^4\text{F})$  ground atomic fragments. This small binding energy value is due to the fact that the main bonding mechanism is a 2c-3e interaction,  $\text{Sc}(4s^2)\text{-}(4s^1)\text{V}$ , supplemented by very weak d-d one or two electron bonds. All septet states correlate adiabatically to the first excited  $\text{Sc}(^2\text{D}) + \text{V}(^6\text{D})$  atomic asymptote. As for the quintets and the triplet states, they all correlate adiabatically to the ground state atoms  $\text{Sc}(^2\text{D}) + \text{V}(^4\text{F})$ . Aside from very shallow van der Waals minima, their global equilibrium electronic configurations correspond to the excited <sup>6</sup>D (quintets) or <sup>4</sup>D (triplets) states of V and are the results of avoided crossings with incoming PECs originating from these channels.

All 25 excited states, presented in this study, are closely packed together within an energy range of less than  $1 \text{ eV}$  with near-degeneracies and quite low binding energies.

As a final remark it is noteworthy to observe the gradual decrease of the adiabatic  $D_e$  values going from Sc<sub>2</sub> to ScTi to ScV. The ground states of these scandium containing diatomic molecules are formed through the same mechanism and they are high spin states, namely,  $\text{Sc}_2(X^5\Sigma_u^-)$ ,  $\text{ScTi}(X^6\Delta)$ ,  $\text{ScV}(X^7\Sigma^+)$ . They correlate adiabatically to the excited  $\text{Sc}(^2\text{D}) + [\text{Sc}(^4\text{F}), \text{Ti}(^5\text{F}), \text{V}(^6\text{D})]$  asymptotes, respectively. Taking data from Ref. [1, 2] and from the present work, we have at the MRCI+Q/cc-pVQZ level:  $D_e = 49.7$  (Sc<sub>2</sub>),  $36.8$  (ScTi),  $25.8$  (ScV) kcal/mol, with a concomitant bond length decrease:  $r_e = 2.75$  (Sc<sub>2</sub>),  $2.66$  (ScTi),  $2.60$  (ScV)  $\text{ \AA}$ . It is plausible to assume that the spatial contraction of the 3d and 4s atomic orbitals, as one goes from Sc to V, [16] is responsible for

these trends.

We conclude this letter with the hope that our results will be helpful in a future investigation of the yet experimentally unexplored ScV system.

### CRediT authorship contribution statement

**Magdalene Liosi:** Writing – original draft, Visualization, Investigation, Formal analysis, Data curation. **Aristotle Papakonfylis:** Writing – review & editing, Writing – original draft, Supervision, Conceptualization.

### Declaration of competing interest

The authors declare that they have no known competing financial interests or personal relationships that could have appeared to influence the work reported in this paper.

### Appendix A. Supplementary data

Supplementary data to this article can be found online at <https://doi.org/10.1016/j.cplett.2025.141977>.

### Data availability

Data will be made available on request.

### References

- [1] A. Kalemos, I.G. Kaplan, A. Mavridis, The Sc<sub>2</sub> dimer revisited, *J. Chem. Phys.* 132 (2010) 024309-1–024309-7, <https://doi.org/10.1063/1.3290951>.
- [2] A. Kalemos, A. Mavridis, All electron ab initio calculations on the ScTi molecule: a really hard nut to crack, *Theor. Chem. Accounts* 132 (2013) 1408.
- [3] A. Kalemos, A. Mavridis, The electronic structure of Ti<sub>2</sub> and Ti<sub>2</sub><sup>+</sup>, *J. Chem. Phys.* 135 (2011) 134302-1–134302-8, <https://doi.org/10.1063/1.3643380>.
- [4] G.L. Gutsev, P. Jena, B.K. Rao, S.N. Khana, Electronic structure and chemical bonding of 3d-metal dimmers ScX, X=Sc-Zn, *J. Chem. Phys.* 114 (2001) 10738–10748, <https://doi.org/10.1063/1.1373693>.
- [5] G.L. Gutsev, M.D. Mochena, P. Jena, C.W. Bauschlicher Jr., H. Partridge III, Periodic table of 3d-metal dimers and their ions, *J. Chem. Phys.* 121 (2004) 6785–6797, <https://doi.org/10.1063/1.1788656>.
- [6] A. Kramida, Y. Ralchenko, J. Reader, NIST ASD Team, NIST Atomic Spectra Database (ver. 5.11) available. <https://physics.nist.gov/asd>, 2024.
- [7] N.B. Balabanov, K.A. Peterson, Systematically convergent basis sets for transition metals I. All electron correlation consistent basis sets for the 3d elements Sc-Zn, *J. Chem. Phys.* 123 (2005) 064107-1–064107-15, <https://doi.org/10.1063/1.1998907>.
- [8] M. Douglas, N.M. Kroll, Quantum electrodynamical corrections to the fine structure of helium, *Ann. Phys.* 82 (1974) 89, [https://doi.org/10.1016/0003-4916\(74\)90333-9](https://doi.org/10.1016/0003-4916(74)90333-9).
- [9] B.A. Hess, Relativistic electronic-structure calculations employing a two-component no-pair formalism with external-field projection operators, *Phys. Rev. A* 33 (1986) 3742, <https://doi.org/10.1103/PhysRevA.33.3742>.
- [10] H.-J. Werner, P.J. Knowles, An efficient internally contracted multiconfiguration-reference CI method, *J. Chem. Phys.* 89 (1988) 5803–5814, <https://doi.org/10.1063/1.455556>.
- [11] M.M.F. de Moraes, Y.A. Aoto, Multi-d-occupancy as an alternative definition for the double d-shell effect, *J. Phys. Chem. A* 127 (2023) 10075–10090, and references therein, <https://doi.org/10.1021/acs.jpca.3c04709>.
- [12] E.R. Davidson, D.W. Silver, Size consistency in the dilute gas helium electronic structure, *Chem. Phys. Lett.* 52 (1977) 403, [https://doi.org/10.1016/0009-2614\(77\)80475-2](https://doi.org/10.1016/0009-2614(77)80475-2).
- [13] H.-J. Werner, P.J. Knowles, et al., Molpro: a quantum chemistry general-purpose program package, *WIREs Comput. Mol. Sci.* 2 (2012) 242–253, <https://doi.org/10.1002/wcms.82>.
- [14] H.-J. Werner, P.J. Knowles, et al., *J. Chem. Phys.* 152 (2020) 144107, <https://doi.org/10.1063/5.0005081>.
- [15] D. Danovich, C. Foroutan-Nejad, P.C. Hiberty, S. Shaik, Nature of the three-electron bond, *J. Phys. Chem. A* 122 (2018) 1873–1885, <https://doi.org/10.1021/acs.jpca.7b11919>.
- [16] C.F. Bunge, J.A. Barrientos, A.V. Bunge, Roothan-Hartree-Fock ground state atomic wavefunctions: slater-type orbital expansions and expectation values for Z=2–54, *At. Data Nucl. Data Tables* 53 (1993) 113–162, <https://doi.org/10.1006/adnd.1993.1003>.
- [17] W. Jiang, N.J. De Yonker, A.K. Wilson, Multireference character for 3d transition-metal-containing molecules, *J. Chem. Theory Comput.* 8 (2012) 460–468, <https://doi.org/10.1021/ct2006852>.